Journal of Power Sources 226 (2013) 266–271

Contents lists available at SciVerse ScienceDirect

Journal of Power Sources

journal homepage: www.elsevier.com/locate/jpowsour

Short communication

Performance of H-shaped membraneless micro fuel cells

Hong Beom Park [a,b], Kyung Heon Lee [a], Hyung Jin Sung [a,*]

[a] Department of Mechanical Engineering, KAIST, 291 Daehak-ro Yuseong-gu, Daejeon 305-701, Korea
[b] Fluid System Design Division, KAERI Daedeokdae-ro, Yuseong-gu, Daejeon 305-353, Korea

HIGHLIGHTS

- Optimal design of H-shaped membraneless micro fuel cells.
- Fabrication and performance test of H-shaped membraneless micro fuel cells.
- High flow rates increase the maximum current density and decrease fuel utilization.
- Performance of membraneless micro fuel cells increases with increasing the reactant concentrations.
- The mixing region in the downstream section of the H-shaped channel is much smaller than that of a rectangular channel.

ARTICLE INFO

Article history:
Received 6 August 2012
Received in revised form
29 October 2012
Accepted 1 November 2012
Available online 10 November 2012

Keywords:
Membraneless micro fuel cell
Mixing region
H-shaped cell
Flow visualization
Current density

ABSTRACT

The geometry of a membraneless micro fuel cell influences reactant mixing and depletion in the downstream section of the cell channel. A small passage restricts the mixing of the anode and cathode fluids in the channel. The optimal design for H-shaped membraneless micro fuel cells has previously been obtained numerically, and in this study is fabricated and tested. The H-shaped design increases the maximum current density, which means that the maximum power density increases. It is also found that high flow rates increase the maximum current density and decrease fuel utilization. The use of different fuels alters the open circuit voltage and thus changes the current density. The maximum current density increases with increases in the reactant concentrations. For visualization of the flow in the H-shaped channel, a polydimethylsiloxane (PDMS) cell is fabricated. The mixing region in the downstream section of the H-shaped channel is much smaller than that in the downstream section of a comparable rectangular channel.

1. Introduction

Membraneless micro fuel cells use liquid reactants (fuel and oxidant) that flow side by side in a single channel. In contrast to conventional fuel cells, membraneless micro fuel cells do not need anode or cathode humidification because the water level in the cell is maintained by the automatic removal of water out of the cell by the channel flow. The structure of membraneless micro fuel cells is simple and easy to miniaturize, so light and stackable fuel cells can be fabricated with MEMS production [1,2]. These advantages mean that membraneless micro fuel cells can be used as an alternative power source for portable devices [2].

There are two major areas of concern in the development of membraneless micro fuel cells: the mixing (diffusion) region and the depletion region. The mixing region is created when the fuel and the oxidant come into contact in the main channel of the cell. When the reactants flow downstream, the diffusion of the reactants increases, mixing increases, and thus fuel crossover increases. The mixing width is usually smaller in the middle of the channel and much larger near the wall, which results in an hourglass-shaped mixing region in the channel [3]. However, if the mixing width increases, the fuel and oxidant move to the opposite electrodes, resulting in higher reactant crossover in the cell, especially in the downstream section of the channel. The main concern about this mixing region is that when fuel or oxidant moves to the opposite electrode, cell performance decreases dramatically even the operation of the cell stops [2].

A depletion region arises when the reactants continuously react at the electrodes' surfaces, which means that in the downstream section of the channel there are fewer reactants available at the electrode. A depletion region also arises when byproducts cover the electrodes' surfaces; as a result, diffusion of the reactants towards the electrodes becomes more difficult. In other words, the concentration gradient is weakened near both electrode surfaces.

* Corresponding author. Tel.: +82 42 350 3027; fax: +82 42 350 5027.
E-mail address: hjsung@kaist.ac.kr (H.J. Sung).

0378-7753/$ – see front matter © 2012 Elsevier B.V. All rights reserved.
http://dx.doi.org/10.1016/j.jpowsour.2012.11.003

For high performance, the reactants should move to the respective electrodes as fast as the reaction rate. In membraneless micro fuel cells, however, the movement of the reactants to the respective electrodes is not as fast as the reaction rate, and this is particularly true of the movement of oxygen to the cathode. As the reactants move downstream, the size of this depletion region increases significantly, which reduces the efficiency of membraneless micro fuel cells. In order to improve cell performance, reductions in the sizes of the mixing and depletion regions are required.

Ferrigno et al. [4] demonstrated membraneless fuel cells for the first time and Choban et al. [2] carried out a preliminary analysis of their fluid dynamics. Bazylak et al. [3] simulated the mixing in a membraneless micro fuel cell with a T-shaped channel. They varied the aspect ratio (width/height), and found that a higher aspect ratio results in a smaller mixing width. Chang et al. [5] performed numerical simulations for various Peclet numbers, and showed that the mixing width decreases as the Peclet number increases. Yoon et al. [6] carried out simulations and experiments with a view to reducing the size of the depletion region, and suggested the use of a Y-channel with many inlets and outlets. Ahmed et al. [7] simulated a membraneless micro fuel cell with a new trident-shape and three inlets. The cross-section of the channel was T-shaped, and a proton-conducting fluid was used in the middle of the channel. Ahmed et al. [8] simulated membraneless micro fuel cells with various geometries and features such as blocks in the channel, as well as butterfly-shaped and octagonal channels. Researchers have also attempted to improve cell performance by using various fuel and oxidant compositions [1,9–13].

An H-shaped design for reducing the size of the mixing region and increasing fuel utilization was proposed by Park et al. [14]. Their numerical results showed that a small passage between the anode and cathode channels reduces the size of the mixing region, reduces reactant crossover, and increases fuel utilization. A low aspect ratio for the anode and cathode channels results in a depletion region of reduced size. The height of the passage has significant influence on the size of the depletion region. If the height of the passage is reduced, the size of the depletion region decreases, the reactants become more confined to their respective channels, and the flux over the electrode and the fuel utilization both increase. In this study, we fabricated an H-shaped membraneless micro fuel cell according to the results of this optimization. The objective of this study was to confirm the performance of this optimized H-shaped membraneless micro fuel cell. The laminar flow of the fuel and oxidant solutions was driven by a syringe pump via Teflon tubing. Formic acid was used as the fuel and potassium permanganate was used as the oxidant. Sulfuric acid was also mixed with the reactants to facilitate the conduction of protons.

2. Optimal design by simulation

Park et al. [14] carried out simulations with a three-dimensional fuel cell model to optimize the design of H-shaped membraneless micro fuel cells. Fig. 1(a) shows a schematic diagram of the H-shaped cell. The fluid flows in the channel and chemical reactions occur on the reaction surfaces. The main goal in the development of the proposed design was to reduce the sizes of the mixing and depletion regions and to increase fuel utilization. Fig. 1(c) and (d) show the contours of the fuel volume fraction in the H-shaped and rectangular cells respectively. When the electrode area (reaction surface) and the mass flow rate of the conventional rectangular design are the same as those of the H-shaped design, the fuel crossover at the cathode electrode of the H-shaped cell is at least 10 times lower (at the far end of the cathode channel) than that of the conventional rectangular geometry. In addition, the size of the

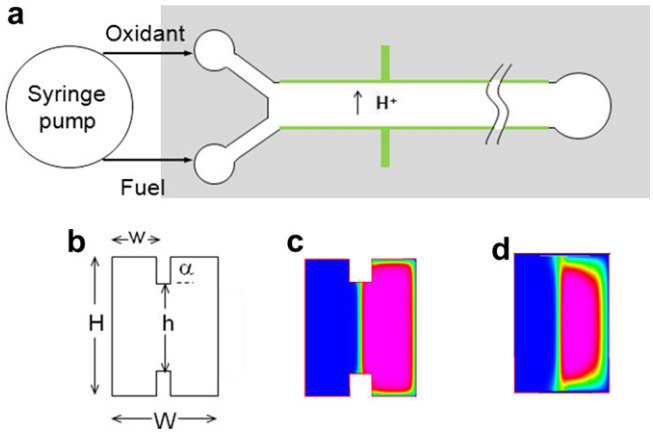

Fig. 1. (a) Schematic diagram of a membraneless fuel cell, (b) cross-section of the cell, (c) contour of the fuel volume fraction of the H-shaped cell, and (d) contour of the fuel volume fraction of the rectangular cell.

mixing region is approximately 20% lower and the fuel utilization approximately 8% higher than those of the rectangular cell. As shown in Fig. 1(b), an angle (α) of 90° between the small passage and the anode and cathode channels optimizes the mixing of the anode and cathode fluids. The low aspect ratio (w/H) of the anode and cathode channels results in a depletion region of reduced size. The fuel utilization of the H-shaped design with an aspect ratio of 0.083 is 23% higher than that of the rectangular design. The height of the passage (h) has a significant influence on the size of the depletion region. If the height of the passage is reduced, the size of the depletion region decreases and the reactants become more confined to their respective channels. Thus, the flux over the electrodes and the fuel utilization increase. The boundary layer thickness gradually increases along the channel, which ultimately results in an increase in the size of the depletion region. This boundary layer thickness is reduced for lower passage heights. Beneath a certain height of the passage, however, there are no further reductions in the size of the depletion region with the proposed H-shaped design. Thus this particular height of the small passage provides the design that optimizes cell performance. The proposed H-shaped design produces smaller mixing and depletion regions and better fuel utilization than the conventional rectangular design. The details of the optimal design can be found in Park et al. [14].

3. Fabrication and experiment

A schematic diagram of the fabrication process is shown in Fig. 2. The micro fluidic channel on a Si wafer was obtained by using standard photolithography and two inductive coupled plasma (ICP) processes. The first step was to coat positive photoresist (AZ5214) at 3000 rpm onto a Si wafer with an oxide layer. The wafer was then baked at 65 °C for 10 min and at 95 °C for 30 min. The wafer was then exposed to the light from an ultraviolet (UV) lamp for 44 s through a mask and postbaked at 65 °C for 3 min and at 95 °C for 10 min. The photoresist was removed from the wafer and reactive ion etching (RIE) was employed to remove the patterned oxide layer. The next step was to coat a positive photoresist at 3000 rpm onto the wafer, which was then baked at 65 °C for 10 min and at 95 °C for 30 min and then exposed again to the UV lamp for 44 s. After postbaking, the photoresist was removed and deep reactive ion etching (DRIE) was performed to depths of 100 μm and 50 μm. One channel and the small passage of the H-shaped design were then fabricated. Next, the fabrication process of the backside was

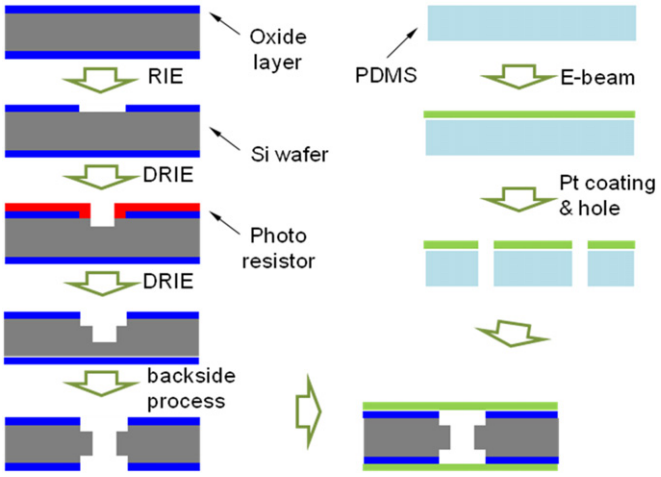

Fig. 2. Schematic diagram of the fabrication process.

repeated as that of the frontside above. The micro electrode on a glass wafer was obtained with a standard E-beam process. The glass wafer was patterned and the electrodes were obtained by using sandblasting and a standard E-beam process with Au/Pt. After removal with acetone, patterned electrodes were obtained. The H-shaped microchannel and electrodes were combined by performing anodic bonding.

For flow visualization, a polydimethylsiloxane (PDMS) fuel cell channel was fabricated. A schematic diagram of the fabrication process is shown in Fig. 3. SU-8 was coated onto a Si wafer at 3000 rpm and baked at 65 °C for 10 min and at 95 °C for 30 min. The wafer was then exposed to the light from a UV lamp for 44 s through a channel patterned mask and postbaked. The wafer was then coated again with SU-8 at 2500 rpm and baked at 65 °C for 16 min. After aligning the channel and small passage patterns, the wafer was exposed to light from a UV lamp for 44 s through the small passage patterned mask and postbaked. SU-8 was then removed with SU-8 remover and room temperature vulcanized (RTV) PDMS (ratio of RTV 3 to RTV hardener 1) was spin-coated. The RTV PDMS was heated at 65 °C for 2 h then removed from the wafer, which finalized the fabrication of the channel and small passage of the H-shaped PDMS microchannel. The other part of the microchannel was fabricated in a similar manner to that used for the RTV PDMS (ratio of RTV 30 to RTV hardener 1). The two parts were bonded with contact at 65 °C for 3 h. Due to different RTV ratio, the RTV PDMS (ratio of RTV 3 to RTV hardener 1) with one channel and a small passage and the RTV PDMS (ratio of RTV 30 to RTV hardener 1) with another part can be bonded. Then the RTV PDMS wafers were made with the RTV and RTV hardener, and the H-shaped PDMS microchannel and the RTV PDMS wafer were bonded at 65 °C for 3 h.

Fig. 4 shows photographs of H-shaped membraneless fuel cells. Fig. 4(a) shows a top view of the H-shaped microchannel. The white regions are the anode and cathode channels. The black region is the small passage. The total width and height are 250 μm and 150 μm, respectively. The width and height of the small passage are 100 μm and 50 μm, respectively. Fig. 4(b) shows multiple electrodes with an H-shaped design. The channel length is 10 mm. As shown in Fig. 1, the laminar flow of the fuel and oxidant solutions required for fuel cell operation is driven by a syringe pump via Teflon tubing. 1 M formic acid was used as the fuel and 1 M potassium permanganate was used as the oxidant. 1 M sulfuric acid was mixed with the fuel and the oxidant for the conduction of protons. Polarization data were obtained at room temperature with a VersaSTAT 3. The current density and power density were calculated according to the active areas of the electrodes.

4. Results and discussion

The polarization and power density curves of the H-shaped cell and the conventional rectangular cell are shown in Fig. 5. Formic acid was used as a fuel and potassium permanganate as an oxidant. The flow rate is 0.01 m s^{-2}. For comparison, the rectangular cell was fabricated with the same process. In Fig. 5(a), the slope of the polarization curve for the rectangular cell is larger than that of the H-shaped cell. The maximum current densities of the H-shaped and rectangular cells are 28 mA cm^{-2} and 16 mA cm^{-2}, respectively. The dimensions of the channel, the flow rate, and the concentrations of the reactants were the same in both simulation and experiment. As shown in Fig. 5, the H-shaped cell exhibits better performance than the rectangular cell. In Fig. 5(b), the maximum power density of the H-shaped cell (13 mW cm^{-2}) is much higher than that of the rectangular cell (7 mW cm^{-2}). The mixing region of the H-shaped cell is smaller than that of the rectangular cell, especially in the downstream section of the channel. The mixing region accounts for approximately 20% of the entire channel. We found in the simulation [14] that fuel crossover in the H-shaped cell is approximately 1% of fuel crossover in the rectangular cell. In the H-shaped cell, the

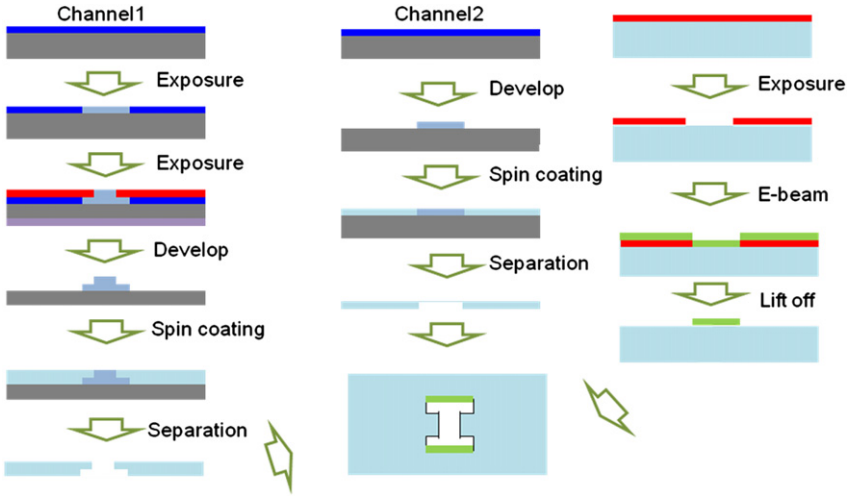

Fig. 3. Schematic diagram of the PDMS fabrication process.

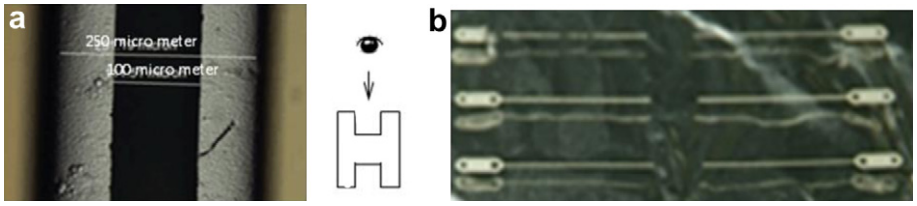

Fig. 4. Photographs of (a) the H-shaped cell and (b) multiple fabricated electrodes.

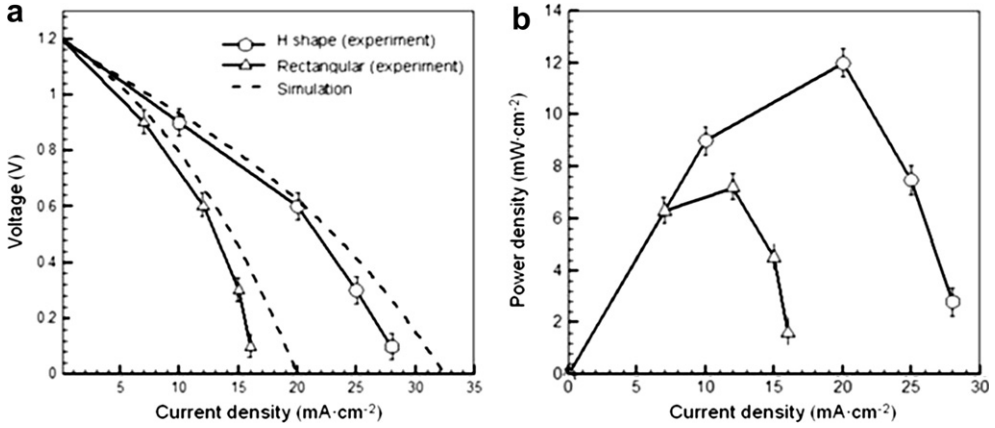

Fig. 5. (a) Polarization curves and (b) power density curves. The flow rate is 0.01 m s^{-2}. Formic acid is used as a fuel and potassium permanganate as an oxidant.

fuel and oxidant remain at each electrode and the depletion region is smaller than that of the rectangular cell, so fuel utilization is improved.

The polarization curves for various inlet reactant velocities and fuels are shown in Fig. 6. Formic acid was used as the fuel and potassium permanganate as the oxidant. The inlet velocities are 0.01 m s^{-1}, 0.05 m s^{-1} and 0.1 m s^{-1}, the corresponding maximum current densities are 28 mA cm^{-2}, 31 mA cm^{-2} and 34 mA cm^{-2}, respectively. The current density increases with increases in the inlet velocity. This trend indicates that the mass transport limitation is significant and that the electrochemical reaction is relatively fast. However, the limiting current density is not proportional to the inlet velocity. Although a stronger convective flow enhances the transport of reactants to the electrodes, this effect gradually diminishes and fuel utilization decreases; thus when the flow rate increases, fuel utilization decreases. Fig. 6(b) shows the polarization curves for various fuels. Membraneless micro fuel cells can use many kinds of fuels (including hydrogen) and oxidants (including oxygen). However, some combinations of fuel and oxidant lead to lower open circuit voltages. Several combinations have been tested. In the present study, formic acid, hydrogen peroxide, and methanol were chosen as the fuels and the open circuit voltages were about 1.2 V, 1.3 V and 1.1 V, respectively. The use of hydrogen peroxide resulted in a maximum open circuit voltage (1.3 V) and a maximum current density (29 mA cm^{-2}). The use of methanol resulted in a minimum open circuit voltage (1.1 V) and a maximum current density (26 mA cm^{-2}). The use of formic acid resulted in an open circuit voltage of 1.2 V and a maximum current density of 28 mA cm^{-2}. The slopes of the polarization curves are similar in the three cases, but the use of hydrogen peroxide results in the largest limiting current density and the largest power density.

The polarization curves for various concentrations of reactants (1 M, 1.5 M, and 2 M) are shown in Fig. 7. The flow rate is 0.01 m s^{-2}, and the maximum current densities are 28 mA cm^{-2}, 30 mA cm^{-2}

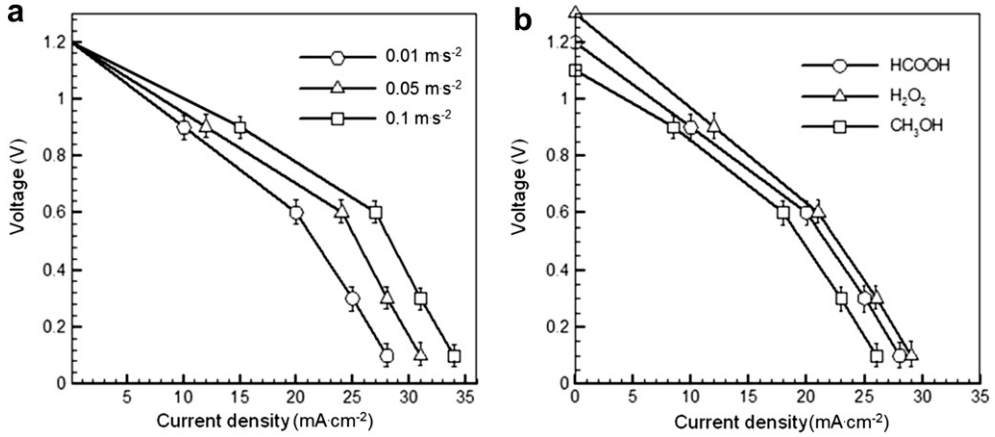

Fig. 6. Polarization curves for (a) various flow rates. Formic acid is used as a fuel and potassium permanganate as an oxidant (b) various fuels. The flow rate is 0.01 m s^{-2} and potassium permanganate is used as an oxidant.

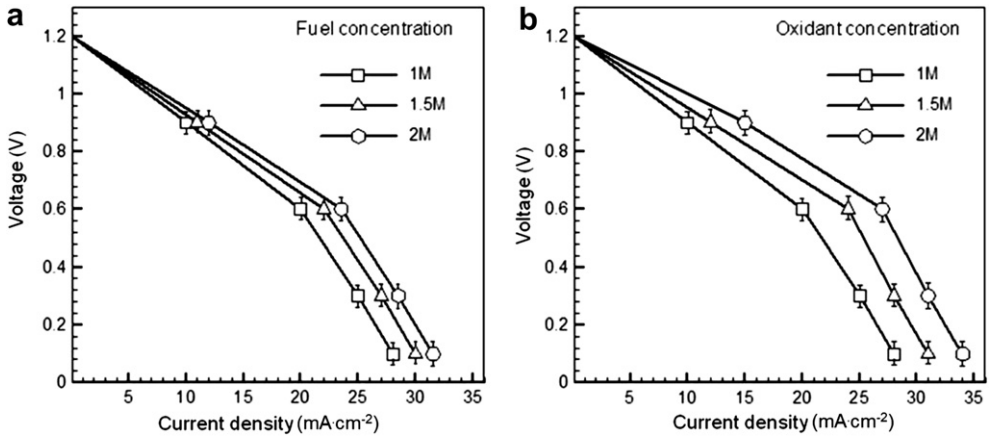

Fig. 7. Polarization curves for (a) various fuel concentrations and (b) various oxidant concentrations. The flow rate is 0.01 m s^{-2}, formic acid is used as a fuel and potassium permanganate as an oxidant.

and 32 mA cm^{-2}, respectively. In general, the open circuit potential is larger at lower concentrations because of reactant crossover. However, the level of reactant crossover in the H-shaped cell is very low. Note also that the higher the fuel concentration, the larger the limiting current density and the larger the maximum power density. As more reactants enter the cell, the mass transport to the electrodes increases. Accordingly, the current density and power density increase. However, the transport rate is limited by the depletion region. The polarization curves for various concentrations of oxidants (1 M, 1.5 M, and 2 M) are shown in Fig. 7(b). The corresponding maximum current densities are 28 mA cm^{-2}, 31 mA cm^{-2}, and 34 mA cm^{-2}, respectively. As in Fig. 7(a), note that the larger the concentration of the oxidant, the better the performance because of the increase in mass transport to the electrodes. When the transport rate reaches its limit and the size of the depletion region increases, performance does not improve. The performance of high concentration of oxidant is better that the performance of high concentration of fuel. Hydrogen proton is from the anode and proton can move faster than potassium permanganate by sulfuric acid that has high proton conductivity. The potassium permanganate can be transported only by diffusion and the diffusion rate is not so high that the cell performance is cathode-limited. This result means that high concentration of the oxidant is more effective in enhancing performance than high concentration of the fuel.

To visualize the mixing and depletion regions, the flows inside the H-shaped and rectangular channels are shown in Fig. 8. 1 M formic acid was used as the fuel and 1 M potassium permanganate was used as the oxidant. 1 M sulfuric acid was mixed with the fuel and the oxidant, and the mixing in the RTV PDMS channel was examined with a microscope. The white region is fuel, the black region is oxidant, and the brown region in the center is the mixing region. The flow visualization for the rectangular cell is also shown for comparison. The mixing region takes up approximately 40% of the entire channel of the H-shaped cell, but approximately 80% of that of the rectangular cell. The size of the mixing region of the H-shaped cell is almost constant in the downstream section. However, the mixing region gradually expands in the downstream section of the rectangular cell. The downstream increase in the width of the mixing region in the rectangular cell is approximately 15 times larger than that of the H-shaped cell. The small passage in the H-shaped cell limits the movement of the reactants, so mixing is reduced. The numerical simulations at the same condition are included for better comparison. As in the simulation, the present experiment has confirmed that the use of an H-shaped channel reduces the size of the mixing region and fuel crossover, which will result in improved performance.

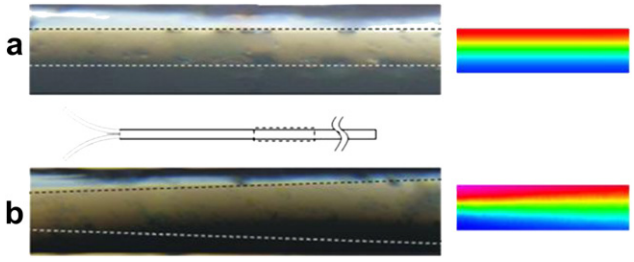

Fig. 8. Flow visualizations for the mixing regions in (a) H-shaped channel and (b) rectangular channel.

5. Conclusions

The optimal H-shaped design was fabricated and tests were carried out to validate the results of previous simulations. The H-shaped cell was fabricated with two ICP MEMS processes. When the polarization curves were examined, it was found that the H-shaped cell exhibits a larger maximum current density than the rectangular cell and a larger maximum power density. Our results confirm the performance predictions of the simulation. The use of high flow rates was found to increase the maximum current density. However, high flow rates also dramatically reduce fuel utilization; fuel efficiency is lower at higher flow rates. The maximum current density increases when the concentrations of the reactants are high. The maximum current density for high concentration of the oxidant was larger than the maximum current density for high concentration of the fuel, because the reaction rate of the oxidant has more influence on performance than the reaction rate of the fuel. The mixing region of the H-shaped cell was found with flow visualization to be smaller in the downstream section than that of the rectangular cell. The proposed H-shaped cell reduces the size of the mixing region and exhibits a higher current density than the rectangular cell.

Acknowledgment

This study was supported by the Creative Research Initiatives (No. 2012-0000246) program of the National Research Foundation of Korea.

References

[1] R.S. Jayashree, L. Gancs, E.R. Choban, A. Primak, D. Natarajan, L.J. Markoski, P.J.A. Kenis, J. Am. Chem. Soc. 127 (2005) 16758–16759.
[2] E.R. Choban, L.J. Markoski, A. Wieckowski, P.J.A. Kenis, J. Power Sources 128 (2004) 54–60.
[3] A. Bazylak, D. Sinton, N. Djilali, J. Power Sources 143 (2005) 57–66. 50(2005) 5390–5398.
[4] R. Ferrigno, A.D. Stroock, T.D. Clark, M. Mayer, G.M. Whitesides, J. Am. Chem. Soc. 124 (2002) 12930–12931.
[5] M.H. Chang, F. Chen, N.S. Fang, J. Power Sources 159 (2006) 810–816.
[6] S.K. Yoon, G.W. Fichtl, P.J.A. Kenis, Lab on a Chip 6 (2006) 1516–1524.
[7] D.H. Ahmed, H.B. Park, H.J. Sung, J. Power Sources 185 (2008) 143–152.
[8] D.H. Ahmed, H.B. Park, K.H. Lee, H.J. Sung, Int. J. Energy Res. (2009). http://dx.doi.org/10.1002/er.1615.
[9] E.R. Choban, J.S. Spendelow, L. Gancs, A. Wieckowski, P.J.A. Kenis, Electrochim. Acta 50 (2005) 5390–5398.
[10] E. Kjeang, B.T. Proctor, A.G. Brolo, D.A. Harrington, N. Djilali, D. Sinton, Electrochim. Acta 52 (2007) 4942–4946.
[11] E. Kjeang, J. McKechnie, D. Sinton, N. Djilali, J. Power Sources 168 (2007) 379–390.
[12] J.L. Cohen, D.J. Volpe, D.A. Westly, A. .Pechenik, H.D. Abruna, Langmuir 21 (2005) 3544–3550.
[13] E. Kjeang, A.G. Brolo, D.A. Harrington, N. Djilali, D. Sinton, J. Electrochem. Soc. 154 (12) (2007) B1220–B1226.
[14] H.B. Park, D.H. Ahmed, K.H. Lee, H.J. Sung, Electrochim. Acta 54 (2009) 4416–4425.